Research Paper

Dual Role of Ninjurin-1 in Myeloid Cell Adhesion and Inflammation in Relapse-Remitting EAE

Coleen Thompson[1], Alex Annett[1], Anastasia Alkhimovitch[2], Kashish Singh Parihar[1], Igal Ifergan[1,2,3]

[1]Department of Molecular and Cellular Biology, College of Medicine, University of Cincinnati, Cincinnati, OH USA.

[2]Division of Immunobiology, Cincinnati Children's Hospital Medical Center, University of Cincinnati College of Medicine, Cincinnati, OH USA

[3]Neuroscience Graduate Program, College of Medicine, University of Cincinnati, Cincinnati, OH USA

Corresponding author:

Igal Ifergan, Ph.D.
Dept. of Molecular and Cellular Biology
College of Medicine
University of Cincinnati
MSB 2258
231 Albert Sabin Way
Cincinnati, OH 45267
E-mail: igal.ifergan@uc.edu
Phone: 513-558-7146

Keywords: Ninjurin-1, EAE, myeloid cells, multiple sclerosis, CNS inflammation

ABSTRACT

Nerve Injury-Induced Protein 1 (Ninjurin-1) is an adhesion molecule implicated in inflammation and tissue injury, yet its role in neuroinflammatory diseases such as multiple sclerosis (MS) remains poorly defined. Here, we identify Ninjurin-1 as a key mediator of immune activation and CNS infiltration in relapsing-remitting experimental autoimmune encephalomyelitis (RR-EAE), a model of relapsing-remitting MS (RRMS). Using flow cytometry, gene-expression profiling, and *in vivo* peptide blockade, we show that Ninjurin-1 is markedly upregulated on CNS-infiltrating myeloid cells during disease progression. Ninjurin-1^{+} myeloid cells display a dual function, as both an adhesion molecule and a marker of inflammatory activation, characterized by increased antigen presentation, cytokine production, and transcriptional enrichment for genes regulating adhesion, migration, and innate immune signaling. Importantly, therapeutic blockade of Ninjurin-1 significantly reduced clinical severity, CNS immune infiltration, and demyelination in RR-EAE. These findings uncover a previously unrecognized role for Ninjurin-1 in myeloid-driven neuroinflammation and highlight its potential as a therapeutic target for relapsing-remitting MS.

1. Introduction

Multiple sclerosis (MS) is a chronic autoimmune disorder affecting over 2.8 million people worldwide, leading to progressive neurological disability and reduced quality of life [1, 2]. The disease is driven by the infiltration of peripheral immune cells into the central nervous system (CNS), where they attack the myelin sheath surrounding neurons, causing demyelination, inflammation, and neurodegeneration [3]. Although the precise etiology of MS remains unclear, a prevailing hypothesis proposes that antigen-presenting cells (APCs) present myelin-mimicking antigens to autoreactive T lymphocytes, thereby initiating immune-mediated demyelination and lesion formation within the CNS [4, 5].

Experimental autoimmune encephalomyelitis (EAE), a well-established preclinical animal model that recapitulates many clinical and pathological features of MS, including limb paralysis, CNS lesions, and immune cell infiltration [6, 7]. EAE studies have identified key roles for TH1 and TH17 $CD4^+$ T cells in driving neuroinflammation and demyelination [8], providing a valuable model to investigate disease mechanisms and test potential therapies.

Immune cell migration into the CNS is orchestrated by a complex interplay of adhesion molecules, chemokines, and selectins expressed by blood–brain barrier endothelial cells (BBB-ECs) and $CD45^+$ immune cells [9]. Among these, vascular cell adhesion molecule-1 (VCAM-1) and intercellular adhesion molecule-1 (ICAM-1) are well-established mediators of leukocyte trafficking in MS and EAE [10]. However, the molecular mechanisms governing immune cell infiltration into the CNS remain incompletely understood, suggesting that additional adhesion pathways contribute to neuroinflammatory progression.

69 One such candidate is Nerve Injury–Induced Protein-1 (Ninjurin-1), a 22-kDa
70 homophilic adhesion molecule originally identified for its role in axonal regeneration
71 following nerve injury [11]. Subsequent work, including a proteomic screen of human
72 BBB-ECs by Ifergan et al. (2013), identified Ninjurin-1 as a molecule expressed at the
73 neurovascular interface and upregulated under inflammatory conditions [12]. Importantly,
74 Ninjurin-1 is also expressed by immune cells, positioning it as a bidirectional mediator of
75 leukocyte-endothelial interactions.

76 More recently, Ninjurin-1 has emerged as a regulator of immune cell adhesion and
77 inflammation across pathological contexts, including stroke [13], pulmonary fibrosis [14],
78 liver ischemia-reperfusion injury [15], and MS [12]. Beyond its adhesive function, Ninjurin-
79 1 promotes leukocyte adhesion, plasma membrane rupture (PMR), and the release of
80 damage-associated molecular patterns (DAMPs) [16], highlighting its potential role in
81 amplifying inflammatory cascades. These findings position Ninjurin-1 as a unique
82 molecule bridging structural adhesion and innate immune activation.

83 In the context of MS and EAE, Ninjurin-1 is expressed in both acute and chronic
84 MS lesions [17] and is upregulated on myeloid and endothelial cells during chronic EAE
85 [12]. Our previous work demonstrated that Ninjurin-1 expression peaks at the height of
86 disease in a chronic EAE model induced by MOG_{35-55}, and that its blockade alleviates
87 clinical symptoms, reduces CNS inflammation, and limits immune cell infiltration [12].
88 Despite these insights, no studies have explored the role of Ninjurin-1 in relapse-remitting
89 EAE (RR-EAE) or its relevance to relapse-remitting MS (RRMS). RRMS is the most
90 prevalent MS subtype, representing approximately 85% of all cases. It is characterized

91 by episodic neuroinflammatory attacks followed by partial recovery, driven by waves of
92 peripheral immune cell infiltration into the CNS [18, 19].

93 In this study, we investigate the expression and function of Ninjurin-1 in RR-EAE.
94 We show that Ninjurin-1 is strongly upregulated in inflammatory environments, particularly
95 on myeloid cells and BBB-ECs, where it functions both as an adhesion molecule and as
96 a marker of inflammation. Furthermore, blockade of Ninjurin-1 homophilic binding
97 attenuates disease severity and reduces immune cell infiltration. Together, these findings
98 identify Ninjurin-1 as a dual-function mediator of immune activation and trafficking in RR-
99 EAE and suggest that targeting Ninjurin-1 may represent a promising therapeutic strategy
100 for RRMS.
101

102 **2. Materials and Methods**

103 *2.1 Mice*

104 Female SJL/J (cat# 000686) and C57BL/6 (cat# 000664) mice from 6-9 weeks old
105 were purchased from The Jackson Laboratory (Bar Harbor, ME). 2D2 mice were bred in-
106 house (originally from The Jackson Laboratory, cat# 006912) and used in experiments
107 once they reached 12-16 weeks old. All CD4+ T cells from 2D2 mice possess a T cell
108 receptor specific (TCR) for MOG_{35-55}. All mice were maintained under specific pathogen-
109 free conditions in the University of Cincinnati's Laboratory Animal Medical Services
110 (LAMS) facility and handled in accordance with AAALAC and IACUC-approved
111 institutional guidelines.

112

113 *2.2 Reagents*

114 Peptides corresponding to the adhesion motif of Ninjurin-1 (amino acids 26-37;
115 sequence PPRWGLRNRPIN) were synthesized and used as a blocking peptide (anti-
116 $Ninj_{26-37}$). A scrambled control peptide (WRGNPGIRWAPH) was also generated for use
117 as a control. Peptides were synthesized by Genemed Biotechnologies Inc. (Torrance,
118 CA).

119

120 *2.3 Active EAE*

121 RR-EAE was induced in 8-10-week-old female SJL/J mice as previously described
122 [20]. Mice received three subcutaneous flank injections (total 100 µL) of $PLP_{139-151}$ peptide
123 (200 µg/mouse; Genemed Biotechnologies Inc.) emulsified in Complete Freund's
124 Adjuvant (BD Biosciences) containing 200 µg of *Mycobacterium tuberculosis* H37Ra. At

125 peak of disease, mice were treated intraperitoneally three times per week with 200 μg of
126 either scrambled peptide or $Ninj_{26–37}$ blocking peptide (1 mg/mL) until the study endpoint
127 (n = 8/group). Clinical scores were recorded daily (0 = asymptomatic; 1 = limp tail; 2 =
128 hind limb weakness; 3 = partial paralysis; 4 = complete paralysis; 5 = moribund). Data
129 are presented as mean ± SEM daily score.
130
131 *2.4 Isolation of splenocytes and CNS*
132 Mice were incapacitated with CO_2 and then perfused with PBS prior to tissue
133 removal, following previously described methods [18]. Spleens were collected at pre-
134 onset, onset, peak, remission, and relapse phases of RR-EAE. Tissue was mechanically
135 dissociated through 100 μm cell strainers and red blood cells were lysed using 0.83%
136 ammonium chloride. Cells were then plated in 96-well plates (0.2-2 x 10^6 cells/well) in
137 RPMI-1640 supplemented with 10% FBS, 2 mM L-glutamine, and 100 U/mL penicillin-
138 streptomycin at 37 °C, 5% CO_2.
139 CNS tissues (brain and spinal cord) were collected at the same time as the spleen
140 and digested with 50 μg/mL DNase I and 500 μg/mL collagenase (Sigma). Mononuclear
141 cells were isolated by 40% Percoll gradient or 20% BSA centrifugation. White blood cells
142 were quantified using a Sysmex XP300 (Horst, IL).
143
144 *2.5 Ex vivo cytokine stimulation*
145 $CD11b^+$ cells were enriched from naïve SJL/J splenocytes using MACS Magnetic
146 separation columns (Miltenyi Biotec) and were plated at 0.5 x 10^6 cells/well in 24 well
147 plates. C57BL/6 brain microvascular endothelial cells (Cell Biologics, C57-6023) were
148 cultured to 90% confluency and then plated at 30,000 cells/well in a 24 well plate. Cells

149 were treated for 24 hours with the following cytokines: GM-CSF (200 ng/mL; R&D), IFN-
150 γ (200 ng/mL; R&D), IL-1β (200 ng/mL; R&D), IL-4 (200 ng/mL; Peprotech), IL-6 (50
151 ng/mL; R&D), IL-10 (200 ng/mL; R&D), IL-17 (200 ng/mL; R&D), TGF-β (200 ng/mL;
152 R&D), or TNF-α (50 ng/mL; R&D). Combination conditions included IFN-γ + TNF-α
153 (referred to as TH1-like) and IL-17 + GM-CSF (referred to as TH17-like). Cytokine
154 concentrations were based on manufacturer-reported ED_{50} values. After the 24-hour
155 incubation (37°C, 5% CO_2), Ninjurin-1 expression was analyzed by flow cytometry.
156
157 *2.6 Flow cytometry staining and analysis*
158 Fc receptors were blocked using anti-mouse CD16/32 (0.25 μg;
159 Thermofisher). Cells were then stained in PBS with fixable LIVE/DEAD reagents (Life
160 Technologies) for 20 minutes in PBS at room temperature in the dark to assess viability.
161 Then cells were stained for surface markers for 20 minutes at 4°C using the specified
162 antibodies (Ninjurin-1 from R&D Systems; all the others from BD Biosciences or
163 Biolegend). When needed, cells were fixed and permeabilized (ThermoFisher) to stain
164 for intracellular markers. To detect T cell cytokine expression, cells were activated for 4
165 hours with 1 mg/ml ionomycin (Iono) and 20 ng/ml phorbol 12-myristate 13-acetate 40
166 (PMA) in the presence of 2 mg/ml brefeldin A (BFA) (Sigma). To detect $CD11b^+$ cytokine
167 expression, cells were activated for 18 hours with 100 ng/ml lipopolysaccharide (LPS)
168 from E. coli serotype 0111:B4 (Sigma) in the presence of 2 mg/ml BFA (Sigma) for the
169 last 2 hours of co-culture. Cells were stained for surface markers and a fixation and
170 permeabilization kit (ThermoFisher) was used. Cells were acquired using a BD
171 FACSCanto II and analyzed using Flowjo version 10.1 software.

172 *2.7 Immunostaining of mouse CNS*

173 CNS tissues from control and RR-EAE mice were fixed in 10% formaldehyde
174 overnight. Luxol Fast Blue (LFB) and hematoxylin and eosin (H&E) staining were
175 performed by the Immunohistochemistry (IHC) Core at the University of Cincinnati.
176 Images were acquired with an EVOS M5000 microscope (Invitrogen) at 10x
177 magnification.

178 For quantification of cellular infiltration in H&E-stained sections, hematoxylin-
179 positive nuclei were manually counted within standardized white matter regions using
180 ImageJ. Three non-overlapping regions of interest (ROIs; 300 × 300 μm each) were
181 analyzed per section, and counts were averaged to generate a single value per section.
182 Values from multiple sections were then averaged to yield one representative value per
183 mouse. Data are expressed as cells per mm^2.

184

185 *2.8 Cell sorting*

186 Splenocytes were removed from naïve C57BL/6 mice and enriched with CD11b
187 magnetic beads from Miltenyi Biotec. Cells were then stained with Ninjurin-1, CD45,
188 CD11b, CD3, B220, Ly6G, and Live Dead antibodies (**Fig. S4**) and sorted into two
189 populations, $CD45^+CD11b^+B220^-CD3^-Ly6G^-Ninjurin\text{-}1^+$ (Ninjurin-1^+) or
190 $CD45^+CD11b^+B220^-CD3^-Ly6G^-Ninjurin\text{-}1^-$ (Ninjurin-1^-) using a MA900 (Sony).

191

192 *2.9 Quantitative PCR*

193 After cell sorting, both populations obtained from cell sorting (Ninjurin-1^+ and
194 Ninjurin-1^-) were lysed using Trizol (Ambion). Purity of the isolated RNA was determined

195 by measuring the ratio of the optical density of the samples at 260/280nm using a
196 Nanodrop spectrophotometer (Thermo Scientific). The OD_{260}/OD_{280} ratio ranged from 1.7
197 to 2.1 for all samples. cDNAs were synthesized using the RT^2 First Strand kit (Qiagen)
198 according to the manufacturer's instructions. The RT^2 Profiler PCR Array Mouse Dendritic
199 and Antigen Presenting Cell (PAMM-406Z) plates were purchased from SABiosciences,
200 Qiagen. This array profiles the expression of 84 genes involved in antigen presentation
201 and includes 5 controls for housekeeping genes, one control for genomic DNA, and three
202 reverse transcription controls. PCRs were performed on a QuantStudio 3 (Thermofisher).
203 The data were analyzed using the web-based software RT^2 Profiler PCR Array data
204 analysis tool (Qiagen). The C_T cut off was 35 and the data was normalized using Beta-2
205 microglobulin (B2m), Heat shock protein 90 alpha (cytosolic), and class B member 1
206 (HSP90ab1) housekeeping genes. Fold-changes for each gene were calculated as the
207 difference in gene expression between the Ninjurin-1^- cells and Ninjurin-1^+ cells. A
208 positive value indicates gene up-regulation, and a negative value indicated gene down-
209 regulation on the Ninjuirin-1^+ cells. Only fold changes of 1.5 or greater were considered
210 in our analysis.
211
212 *2.8 2D2 Co-culture*
213 Splenocytes were isolated from 2D2 mice, and $CD4^+$ cells were magnetically
214 separated via a negative $CD4^+$ selection kit (Stemcell) and then labeled with
215 carboxyfluorescein succinimidyl ester (CFSE) (Invitrogen). $CFSE^+CD4^+$ T cells
216 (100,000/well) were then co-cultured with either Ninjurin-1^- or Ninjurin-1^+ sorted cells
217 (40,000/well) with 20 μg/ml MOG_{35-55} peptide (Genemed Biotechnologies Inc.) into a 96

218 well plate for 72 hours. After 72 hours, PMA/Iono/BFA was added for 4 hours to the culture
219 prior to cell staining. The expression of CFSE, CD25, GM-CSF, IL-17, IFNγ, and TNF-α
220 on T cells was analyzed via flow cytometry.
221
222 *2.9 Statistical analysis*
223 Statistical analyses were performed using GraphPad PRISM 10.0 (GraphPad
224 software). Data are presented as the mean $\pm$ the standard error of the mean (SEM). EAE
225 scores were analyzed by nonparametric Mann-Whitney test. All other analyses were
226 performed by a paired t- test or a two-way Anova. Only p values < 0.05 were considered
227 significant.
228

229 **3. Results**

230 *3.1 Myeloid cells upregulate Ninjurin-1 expression in the CNS during RR-EAE*

231 We sought to determine whether Ninjurin-1 played a role in RR-EAE, a mouse
232 model of RRMS, as this had not been previously investigated. To assess the dynamics
233 of Ninjurin-1 expression over the course of RR-EAE, we analyzed immune cells isolated
234 from the CNS (brain and spinal cord) and spleen using flow cytometry at defined disease
235 stages: pre-onset (days 7-9), onset (days 11-13), peak (days 14-16), remission (days 21-
236 23), and relapse (days 28-32) (**Fig. 1A**). RR-EAE was induced in female SJL/J mice with
237 $PLP_{139-151}$. Our analysis focused on $CD11b^+$ myeloid cells and $CD3^+$ T cells, the principal
238 immune cell populations infiltrating the CNS during RR-EAE [21-23]. The gating strategy
239 can be found be found in (**Fig. S1)**.

240 Across all disease phases, Ninjurin-1 expression was significantly higher on
241 infiltrating CNS myeloid cells ($CD45^{hi}B220^-CD3^-CD11b^+$) compared to peripheral
242 myeloid cells in the spleen (**Fig. 1B**). Specifically, Ninjurin-1^+ myeloid cells accounted for
243 29% versus 12% at pre-onset, 52% versus 6% at onset, 57% versus 9% at peak, 32%
244 versus 5% at remission, and 36% versus 12% at relapse of the total myeloid cells
245 recorded (CNS vs. spleen, respectively). This enrichment suggests that Ninjurin-1^+ cells
246 may preferentially migrate to or upregulate Ninjurin-1 expression within the CNS
247 microenvironment.

248 In contrast, $CD3^+$ T cells ($CD45^{hi}B220^-CD11b^-CD3^+$) exhibited consistently low
249 Ninjurin-1 expression throughout RR-EAE, with no significant differences between CNS
250 (3.1 ± 1.5%) and spleen (1.7 ± 1.0%) compartments (**Fig. 1C**).

251 Together, these results demonstrate that Ninjurin-1 is predominantly expressed by
252 CNS-infiltrating myeloid cells during RR-EAE, with maximal expression observed at
253 disease onset and peak of disease (**Fig. 1D**). These findings identify Ninjurin-1 as a
254 potential marker of inflammatory myeloid cell activation within the CNS during
255 neuroinflammatory progression.
256
257 *3.2 CD4$^+$ TH17- and TH1-like conditions increase Ninjurin-1 expression in both BBB*
258 *endothelial and myeloid cells*
259 Having observed elevated Ninjurin-1 expression on CNS infiltrating myeloid cells,
260 we next investigated the environmental cues that regulate its expression. We previously
261 demonstrated that Ninjurin-1 plays a role in mediating myeloid cell binding to BBB-ECs
262 through homophilic binding [12]. T helper cells, especially TH1 and TH17 subsets, are
263 known to promote inflammation and promote adhesion molecules through their cytokine
264 release in EAE/MS [21, 22, 24], we sought to determine whether cytokines associated
265 these T helper subsets could modulate Ninjurin-1 expression on either BBB-ECs and
266 myeloid cells.
267 Primary mouse BBB-ECs and splenic CD45$^+$CD11b$^+$ myeloid cells were incubated
268 for 24 hours under resting conditions or stimulated with individual cytokines: GM-CSF,
269 IFN-γ, IL-1β, IL-4, IL-6, IL-10, IL-17, TGF-β, or TNF-α, or under combined TH1-like (IFN-
270 γ + TNF-α) and TH17-like (IL-17 + GM-CSF) conditions. Ninjurin-1 expression was
271 quantified by flow cytometry relative to resting cells.
272 On BBB-ECs, only the TH1- and TH17-like conditions significantly increased
273 Ninjurin-1 expression, rising from 13.6% in resting cells to 24.8% and 21.7%, respectively

274 (n = 5; **Fig. 2A**). Similarly, CD11b^{+} myeloid cells isolated from naïve spleens showed
275 marked upregulation of Ninjurin-1 under GM-CSF (14.3%; **p < 0.01), TNF-α (16.1%;
276 ***p < 0.001), TH1-like (13.2%; **p < 0.01), and TH17-like (14.9%; ***p < 0.001)
277 conditions compared to resting cells (8.6%; n = 6; **Fig. 2B**). Other cytokines had no
278 significant effect on Ninjurin-1 expression in either BBB-ECs or myeloid cells.

279 These results align with our previous observations in human BBB-ECs [12], where
280 IFN-γ and TNF-α induced Ninjurin-1 upregulation. Because TH1 and TH17 cytokines are
281 key inflammatory mediators in EAE and MS [24], these findings suggest that cytokine-
282 rich environments characteristic of the inflamed CNS drive Ninjurin-1 upregulation on both
283 endothelial and myeloid cells, potentially facilitating immune cell adhesion and
284 recruitment across the BBB.

285

286 *3.3 Ninjurin-1^{+} myeloid cells exhibit enhanced co-stimulatory and pro-inflammatory*
287 *profiles in vivo.*

288 Given the elevated expression of Ninjurin-1 on CNS infiltrating myeloid cells and
289 their established role in EAE pathology, we next compared the phenotypic and functional
290 characteristics of Ninjurin-1^{+} and Ninjurin-1^{-} myeloid populations. Immune cells were
291 isolated from the CNS and spleen of EAE mice at disease onset (day 11-13) when
292 Ninjurin-1 expression was maximal in the CNS (**Fig. 1D**).

293 Flow cytometric analysis revealed that CD45^{hi}CD11b^{+}Ninjurin-1^{+} myeloid cells
294 from the CNS expressed significantly higher levels of the co-stimulatory molecules CD80
295 and CD86, as well as MHC II, compared with their Ninjurin-1^{-} counterparts (**Fig. 3A**; n =
296 5). A similar upregulation of these activation markers was also observed in splenic

297 CD11b$^+$Ninjurin-1$^+$ cells (**Fig. S2A**). PD-L1 expression did not differ significantly between
298 Ninjurin-1$^+$ and Ninjurin-1$^-$ populations in either compartment.

299 We next assessed the expression of inflammatory cytokines associated with TH1
300 and TH17 polarization, including TNF-α, IL-1β, IL-12p40, and IL-23p19. In the CNS,
301 Ninjurin-1$^+$ myeloid cells expressed significantly higher levels of TNF-α, IL-1β, and IL-
302 12p40 than Ninjurin-1$^-$ cells (**Fig. 3B**). In the spleen, Ninjurin-1$^+$ myeloid cells also
303 exhibited increased expression of IL-1β, IL-6, IL-12p40, IL-23p19, TGF-β, and TNF-α
304 (**Fig. S2B**).

305 Together, these findings indicate that Ninjurin-1$^+$ myeloid cells display a
306 heightened activation state characterized by elevated co-stimulatory molecule expression
307 and robust production of pro-inflammatory cytokines. This phenotype suggests an
308 enhanced capacity of Ninjurin-1$^+$ cells to promote T-cell activation and sustain CNS
309 inflammation during RR-EAE.

310

311 *3.4 Ninjurin-1$^+$ CD11b$^+$Ly6G$^-$ splenocytes exhibit differential expression of antigen-*
312 *presentation and inflammatory genes*

313 Given the marked differences in co-stimulatory molecule and cytokine expression
314 between Ninjurin-1$^+$ and Ninjurin-1$^-$ myeloid cells, we next investigated whether these
315 populations possess distinct transcriptional profiles independent of disease context. To
316 this end, CD45$^+$CD11b$^+$B220$^-$CD3$^-$Ly6G$^-$Ninjurin-1$^+$ and
317 CD45$^+$CD11b$^+$B220$^-$CD3$^-$Ly6G$^-$Ninjurin-1$^-$ splenocytes were flow-sorted from naïve
318 mice (gating shown in **Fig. S3**). RNA was extracted, converted to cDNA, and subjected

319 to targeted qPCR profiling of genes involved in antigen presentation and innate immune
320 activation.

321 Overall, the transcriptional data support the hypothesis that Ninjurin-1$^+$ myeloid
322 cells are intrinsically more pro-inflammatory than their Ninjurin-1$^-$ counterparts. Genes
323 associated with antigen presentation and immune activation, including Tnf, Cd40, H2-
324 DMa, and Relb, were significantly upregulated in Ninjurin-1$^+$ cells (**Table 1**). Enhanced
325 expression of Tlr1 and Tlr7 further indicates increased responsiveness to innate immune
326 stimuli. In parallel, elevated expression of adhesion and migration molecules such as
327 Icam1 and Cd44 suggests that Ninjurin-1$^+$ cells are well equipped to traffic to and interact
328 with inflamed tissues, reinforcing their potential role in amplifying CNS inflammation.

329 Interestingly, several chemokines involved in leukocyte recruitment, including
330 Ccl3, Ccl4, and Ccl5 (RANTES), were downregulated, whereas Cxcl10 (IP-10) was
331 upregulated, indicating a shift toward a more selective chemokine profile that may favor
332 specific immune-cell interactions within inflammatory microenvironments.

333 Collectively, these transcriptional data indicate that Ninjurin-1 expression defines
334 a subset of myeloid cells with heightened antigen-presenting capacity, migratory
335 potential, and pro-inflammatory gene expression, positioning Ninjurin-1 as both a
336 functional adhesion molecule and a marker of inflammatory myeloid activation.

337

338 *3.5 Ninjurin-1$^+$ myeloid cells enhance activation and proliferation of MOG$_{35-55}$-specific*
339 *CD4$^+$ T cells*

340 Building on our previous findings, we hypothesized that Ninjurin-1$^+$ myeloid cells
341 act as more potent antigen-presenting cells (APCs), leading to stronger CD4$^+$ T cell

342 activation. To test this, we co-cultured FACS-sorted Ninjurin-1$^+$ or Ninjurin-1$^-$ myeloid
343 cells with MOG_{35-55} peptide (20 μg/ml) and CFSE-labeled CD4$^+$ T cell isolated from 2D2
344 transgenic mice, which express a T cell receptor specific for MOG_{35-55}. 2D2 T cells were
345 also cultured with MOG_{35-55} with no myeloid cells and co-cultured with myeloid cells
346 without MOG_{35-55} as controls. After 72 hours of co-culture, T cell proliferation and
347 phenotype was assessed by CFSE dilution and expression of CD25, IL-17, GM-CSF,
348 IFN-γ, and TNF-α.

349 CD4$^+$ T cells co-cultured with Ninjurin-1$^+$ APCs displayed markedly greater
350 proliferation compared to those cultured with Ninjurin-1$^-$ cells (**Fig. 4A**). This enhanced
351 proliferation was accompanied by increased CD25 expression, consistent with elevated
352 T cell activation (**Fig. 4B**). Furthermore, cytokine profiling revealed that CD4$^+$ T cells
353 stimulated by Ninjurin-1$^+$ APCs produced higher levels of TNF-α (**Fig. 4B**), suggesting a
354 stronger pro-inflammatory response.

355 Together, these results demonstrate that Ninjurin-1$^+$ myeloid cells exhibit superior
356 antigen-presenting capacity and promote a more robust and inflammatory CD4$^+$ T cell
357 response, further supporting their role as key drivers of neuroinflammation during EAE.

358

359 *3.6 Anti-Ninjurin-1 treatment at peak disease ameliorates RR-EAE*

360 Given that Ninjurin-1 remains highly expressed in the CNS throughout all phases
361 of RR-EAE, we next tested whether blocking its function could modify disease
362 progression. To this end, SJL/J mice were treated intraperitoneally with 1 mg/mL of the
363 anti-Ninjurin-1_{26-37} blocking peptide or a scramble control three times per week, beginning
364 at the peak of disease (~day 15). Mice were monitored and disease severity was scored

365 daily until day 30, at which point the CNS was harvested for histological and flow
366 cytometric analyses.

367 Mice treated with anti-Ninjurin-1 displayed significantly lower clinical scores and
368 were largely protected from relapse, indicating a marked improvement in disease
369 outcome (**Fig. 5A**). Consistent with the known role of Ninjurin-1 as an adhesion molecule,
370 its blockade resulted in a substantial reduction in immune cell infiltration into the CNS,
371 including total $CD45^+$ leukocytes, $CD3^+$ and $CD4^+$ T cells, $B220^+$ B cells, and $CD11b^+$
372 myeloid cells (**Fig. 5B**).

373 Histological assessment at the end of treatment confirmed these findings, as spinal
374 cord sections from anti-Ninjurin-1-treated mice exhibited fewer immune cell infiltrates
375 compared to controls (**Fig. 5C**). Quantification of cellular infiltration in H&E-stained spinal
376 cord sections revealed a significant reduction in anti-Ninjurin-1-treated EAE mice
377 compared with controls, as assessed by nuclear density within standardized white matter
378 regions (**Fig. 5D**; cells/mm^2; n = 3 mice per group). These results are consistent with
379 previous studies reporting reduced APC infiltration in chronic EAE following Ninjurin-1
380 blockade, supporting a role for Ninjurin-1 in mediating immune cell adhesion and
381 trafficking into the CNS.

382 Together, these findings demonstrate that therapeutic blockade of Ninjurin-1
383 ameliorates RR-EAE when administered at peak disease, at least in part by limiting CNS
384 immune infiltration and inflammation, thereby supporting Ninjurin-1 as a promising
385 immunomodulatory target for relapsing-remitting MS.

386 **4. Discussion**

387 This study identifies Ninjurin-1 as a critical regulator of neuroinflammation in RR-
388 EAE, revealing its dual roles as both an adhesion molecule and a marker of inflammatory
389 activation in myeloid cells. We show that Ninjurin-1 expression is markedly upregulated
390 in the CNS during active disease and that its blockade mitigates immune infiltration and
391 clinical severity. These findings establish Ninjurin-1 as a previously unrecognized
392 mediator linking peripheral immune activation to central neuroinflammation.

393 Our data demonstrates that Ninjurin-1 expression defines a population of myeloid
394 cells with enhanced pro-inflammatory and antigen-presenting functions. Ninjurin-1^{+}
395 myeloid cells exhibited higher expression of MHC II and co-stimulatory molecules,
396 increased production of cytokines such as TNF-α and IL-1β, and a distinct transcriptional
397 profile enriched for genes associated with antigen presentation, Toll-like receptor
398 signaling, and cell adhesion. The upregulation of Tlr1 and Tlr7 in these cells is particularly
399 relevant, as both receptors have been implicated in MS and EAE [25, 26]. Activation of
400 TLR1 enhances microglial and macrophage responsiveness to bacterial lipoproteins and
401 misfolded proteins, and promotes pro-inflammatory cytokine release [27, 28], while TLR7
402 stimulation induces type I interferons and TNF-α, contributing to CNS inflammation and
403 demyelination [29, 30]. Thus, Ninjurin-1^{+} cells may represent a population highly
404 responsive to TLR-driven inflammatory cues within the CNS, further amplifying innate and
405 adaptive immune activation. Together, these transcriptional changes outline a
406 multifaceted activation program in Ninjurin-1^{+} myeloid cells that integrates innate sensing,
407 adhesion, and cytokine signaling.

408 The concurrent upregulation of Icam1 and Cd44 suggests that these cells are
409 primed for tissue infiltration and sustain interaction with other immune cells within the
410 inflamed CNS. Interestingly, Cxcl10 (IP-10), a chemokine known to recruit CXCR3$^+$ Th1
411 cells across the BBB [31], was also increased in Ninjurin-1$^+$ myeloid cells. Elevated
412 CXCL10 levels have been observed in active MS lesions and in EAE, where they promote
413 the accumulation of pathogenic T cells and perpetuate the inflammatory milieu [32, 33].
414 These features parallel pathogenic myeloid subsets identified in MS lesions, which have
415 been shown to drive demyelination and neurodegeneration [34-37], and support a model
416 in which Ninjurin-1$^+$ myeloid cells drive lesion formation and disease progression through
417 both antigen presentation and chemokine-mediated immune recruitment.

418 Importantly, we found that TH1- and TH17-associated cytokines, including IFN-γ,
419 TNF-α, GM-CSF, and IL-17 induce Ninjurin-1 expression on both BBB-ECs and myeloid
420 cells. This places Ninjurin-1 downstream of key inflammatory pathways known to
421 dominate during MS relapses. Such cytokine-driven upregulation provides a mechanistic
422 link between systemic immune activation and localized BBB disruption, where Ninjurin-1
423 may facilitate leukocyte adhesion and transmigration. The observed upregulation of
424 Ninjurin-1 on both endothelial and infiltrating myeloid cells supports the concept of
425 homophilic interactions across the BBB, potentially stabilizing immune cell adhesion and
426 promoting CNS entry.

427 Therapeutic blockade of Ninjurin-1 at the peak of disease attenuated clinical
428 scores, reduced immune cell infiltration, and decreased CNS inflammation. This effect
429 resembles the efficacy of adhesion-molecule inhibitors such as Natalizumab, which
430 targets α4-integrin/VCAM-1 interactions [38]. However, Ninjurin-1's unique dual role

431 distinguishes it from canonical adhesion molecules. Unlike ICAM-1 and VCAM-1, which
432 primarily mediate leukocyte-endothelial interactions, Ninjurin-1 exerts a dual influence by
433 functioning both on vascular and immune compartments. Its homophilic binding supports
434 leukocyte adhesion at the BBB, while its intracellular signaling capacity enhances myeloid
435 activation and antigen presentation within the CNS. This combination positions Ninjurin-
436 1 as both a structural and signaling mediator of neuroinflammation, extending its role
437 beyond passive adhesion to active immune modulation.

438 Beyond its adhesive role, Ninjurin-1 may also influence inflammatory cell survival
439 and signaling. Previous reports have implicated Ninjurin-1 in plasma membrane rupture
440 and the subsequent release of damage-associated molecular patterns [16, 39, 40],
441 processes that can propagate sterile inflammation. Together with our findings, this raises
442 the possibility that Ninjurin-1 contributes to a feed-forward loop wherein inflammatory
443 cytokines induce its expression, promoting adhesion, activation, and additional cytokine
444 release that sustain neuroinflammation.

445 Our findings extend the understanding of adhesion molecules in MS by
446 emphasizing immune cell-intrinsic regulation rather than endothelial expression alone. By
447 integrating cytokine signaling, adhesion, and immune activation, Ninjurin-1 bridges
448 molecular pathways that have traditionally been studied in isolation. Given that Ninjurin-
449 1 is upregulated in multiple inflammatory conditions, including stroke and fibrosis, its role
450 may not be limited to demyelinating disease but may represent a broader mechanism of
451 leukocyte-mediated tissue injury.

452 In conclusion, we identify Ninjurin-1 as a novel adhesion and activation molecule
453 driving myeloid-mediated inflammation in RR-EAE. Through its induction by TH1/TH17

454 cytokines and expression on both BBB-endothelial and immune cells, Ninjurin-1
455 orchestrates key steps in immune cell recruitment and activation within the CNS. Its
456 blockade alleviates disease even at advanced stages, underscoring its therapeutic
457 potential. Future studies should assess Ninjurin-1 expression in human MS lesions and
458 determine whether its signaling partners and downstream pathways can be targeted to
459 modulate disease progression. Elucidating the intracellular signaling cascades engaged
460 by Ninjurin-1 will be essential to understand how this molecule bridges adhesion and
461 immune activation, and may uncover new opportunities for therapeutic intervention.
462
463
464 **Author Contributions**
465 C.T. conducted most the experiments. A.Annett assisted with EAE studies. C.T., A.
466 Alkhimovitch, and K.S.P had intellectual input and revised the manuscript. I.I. supervised
467 the project and revised the manuscript. All authors contributed to manuscript preparation.
468
469 **Acknowledgments**
470 I.I. is supported by the National Institutes of Health (NIH) through an R35 Maximizing
471 Investigators' Research Award (R35GM146890) and an R03 grant (R03NS144870). We
472 thank the University of Cincinnati's histology core and the Laboratory Animal Medical
473 Services (LAMS), as well as Cincinnati Children's Hospital flow cytometry core for
474 technical support.
475
476 **Conflict of interest:** The authors declare no conflict of interest.

REFERENCES

1. Walton C, King R, Rechtman L, Kaye W, Leray E, Marrie RA, et al. Rising prevalence of multiple sclerosis worldwide: Insights from the Atlas of MS, third edition. Mult Scler. 2020;26(14):1816-21. Epub 2020/11/12. doi: 10.1177/1352458520970841. PubMed PMID: 33174475; PubMed Central PMCID: PMCPMC7720355.

2. Amtmann D, Bamer AM, Kim J, Chung H, Salem R. People with multiple sclerosis report significantly worse symptoms and health related quality of life than the US general population as measured by PROMIS and NeuroQoL outcome measures. Disabil Health J. 2018;11(1):99-107. Epub 2017/04/27. doi: 10.1016/j.dhjo.2017.04.008. PubMed PMID: 28442320.

3. Filippi M, Bar-Or A, Piehl F, Preziosa P, Solari A, Vukusic S, et al. Multiple sclerosis. Nat Rev Dis Primers. 2018;4(1):43. Epub 2018/11/10. doi: 10.1038/s41572-018-0041-4. PubMed PMID: 30410033.

4. Rojas M, Restrepo-Jimenez P, Monsalve DM, Pacheco Y, Acosta-Ampudia Y, Ramirez-Santana C, et al. Molecular mimicry and autoimmunity. J Autoimmun. 2018;95:100-23. Epub 2018/12/05. doi: 10.1016/j.jaut.2018.10.012. PubMed PMID: 30509385.

5. Boutitah-Benyaich I, Eixarch H, Villacieros-Alvarez J, Hervera A, Cobo-Calvo A, Montalban X, et al. Multiple sclerosis: molecular pathogenesis and therapeutic intervention. Signal Transduct Tar. 2025;10(1). doi: ARTN 324 10.1038/s41392-025-02415-4. PubMed PMID: WOS:001585285900003.

499 6. Lovett-Racke AE. Contribution of EAE to understanding and treating multiple
500 sclerosis. J Neuroimmunol. 2017;304:40-2. Epub 2016/08/22. doi:
501 10.1016/j.jneuroim.2016.08.013. PubMed PMID: 27544641.

502 7. Dedoni S, Scherma M, Camoglio C, Siddi C, Dazzi L, Puliga R, et al. An overall
503 view of the most common experimental models for multiple sclerosis. Neurobiol Dis.
504 2023;184:106230. Epub 2023/07/16. doi: 10.1016/j.nbd.2023.106230. PubMed PMID:
505 37453561.

506 8. Attfield KE, Jensen LT, Kaufmann M, Friese MA, Fugger L. The immunology of
507 multiple sclerosis. Nat Rev Immunol. 2022;22(12):734-50. Epub 2022/05/05. doi:
508 10.1038/s41577-022-00718-z. PubMed PMID: 35508809.

509 9. Engelhardt B, Ransohoff RM. Capture, crawl, cross: the T cell code to breach the
510 blood-brain barriers. Trends Immunol. 2012;33(12):579-89. Epub 2012/08/29. doi:
511 10.1016/j.it.2012.07.004. PubMed PMID: 22926201.

512 10. Ransohoff RM, Engelhardt B. The anatomical and cellular basis of immune
513 surveillance in the central nervous system. Nat Rev Immunol. 2012;12(9):623-35. Epub
514 2012/08/21. doi: 10.1038/nri3265. PubMed PMID: 22903150.

515 11. Araki T, Milbrandt J. Ninjurin, a novel adhesion molecule, is induced by nerve
516 injury and promotes axonal growth. Neuron. 1996;17(2):353-61. Epub 1996/08/01. doi:
517 10.1016/s0896-6273(00)80166-x. PubMed PMID: 8780658.

518 12. Ifergan I, Kebir H, Terouz S, Alvarez JI, Lecuyer MA, Gendron S, et al. Role of
519 Ninjurin-1 in the migration of myeloid cells to central nervous system inflammatory

520 lesions. Ann Neurol. 2011;70(5):751-63. Epub 2011/12/14. doi: 10.1002/ana.22519.
521 PubMed PMID: 22162058.

522 13. Dong N, Wu X, Hong T, Shen X, Guo X, Wang H, et al. Elevated Serum Ninjurin-
523 1 Is Associated with a High Risk of Large Artery Atherosclerotic Acute Ischemic Stroke.
524 Transl Stroke Res. 2023;14(4):465-71. Epub 2022/10/08. doi: 10.1007/s12975-022-
525 01077-6. PubMed PMID: 36205878.

526 14. Choi S, Woo JK, Jang YS, Kang JH, Hwang JI, Seong JK, et al. Ninjurin1 Plays a
527 Crucial Role in Pulmonary Fibrosis by Promoting Interaction between Macrophages and
528 Alveolar Epithelial Cells. Sci Rep. 2018;8(1):17542. Epub 2018/12/05. doi:
529 10.1038/s41598-018-35997-x. PubMed PMID: 30510259; PubMed Central PMCID:
530 PMCPMC6277454.

531 15. Hu Y, Zhan F, Wang Y, Wang D, Lu H, Wu C, et al. The Ninj1/Dusp1 Axis
532 Contributes to Liver Ischemia Reperfusion Injury by Regulating Macrophage Activation
533 and Neutrophil Infiltration. Cell Mol Gastroenterol Hepatol. 2023;15(5):1071-84. Epub
534 2023/02/03. doi: 10.1016/j.jcmgh.2023.01.008. PubMed PMID: 36731792; PubMed
535 Central PMCID: PMCPMC10036740.

536 16. Kayagaki N, Kornfeld OS, Lee BL, Stowe IB, O'Rourke K, Li Q, et al. NINJ1
537 mediates plasma membrane rupture during lytic cell death. Nature.
538 2021;591(7848):131-6. Epub 2021/01/21. doi: 10.1038/s41586-021-03218-7. PubMed
539 PMID: 33472215.

540 17. Tajouri L, Fernandez F, Griffiths LR. Gene expression studies in multiple
541 sclerosis. Curr Genomics. 2007;8(3):181-9. Epub 2008/07/23. doi:
542 10.2174/138920207780833829. PubMed PMID: 18645602; PubMed Central PMCID:
543 PMCPMC2435352.

544 18. Frischer JM, Weigand SD, Guo Y, Kale N, Parisi JE, Pirko I, et al. Clinical and
545 pathological insights into the dynamic nature of the white matter multiple sclerosis
546 plaque. Ann Neurol. 2015;78(5):710-21. Epub 2015/08/05. doi: 10.1002/ana.24497.
547 PubMed PMID: 26239536; PubMed Central PMCID: PMCPMC4623970.

548 19. Charabati M, Wheeler MA, Weiner HL, Quintana FJ. Multiple sclerosis:
549 Neuroimmune crosstalk and therapeutic targeting. Cell. 2023;186(7):1309-27. Epub
550 2023/04/01. doi: 10.1016/j.cell.2023.03.008. PubMed PMID: 37001498; PubMed
551 Central PMCID: PMCPMC10119687.

552 20. Ifergan I, Davidson TS, Kebir H, Xu D, Palacios-Macapagal D, Cann J, et al.
553 Targeting the GM-CSF receptor for the treatment of CNS autoimmunity. J Autoimmun.
554 2017;84:1-11. Epub 2017/06/24. doi: 10.1016/j.jaut.2017.06.005. PubMed PMID:
555 28641926; PubMed Central PMCID: PMCPMC5647260.

556 21. Becher B, Spath S, Goverman J. Cytokine networks in neuroinflammation. Nat
557 Rev Immunol. 2017;17(1):49-59. Epub 2016/12/06. doi: 10.1038/nri.2016.123. PubMed
558 PMID: 27916979.

559 22. Becher B, Derfuss T, Liblau R. Targeting cytokine networks in neuroinflammatory
560 diseases. Nat Rev Drug Discov. 2024;23(11):862-79. Epub 2024/09/12. doi:
561 10.1038/s41573-024-01026-y. PubMed PMID: 39261632.

562 23. King IL, Dickendesher TL, Segal BM. Circulating Ly-6C+ myeloid precursors
563 migrate to the CNS and play a pathogenic role during autoimmune demyelinating
564 disease. Blood. 2009;113(14):3190-7. Epub 2009/02/07. doi: 10.1182/blood-2008-07-
565 168575. PubMed PMID: 19196868; PubMed Central PMCID: PMCPMC2665891.

566 24. Krishnarajah S, Becher B. T(H) Cells and Cytokines in Encephalitogenic
567 Disorders. Front Immunol. 2022;13:822919. Epub 2022/03/25. doi:
568 10.3389/fimmu.2022.822919. PubMed PMID: 35320935; PubMed Central PMCID:
569 PMCPMC8934849.

570 25. Zheng C, Chen J, Chu F, Zhu J, Jin T. Inflammatory Role of TLR-MyD88
571 Signaling in Multiple Sclerosis. Front Mol Neurosci. 2019;12:314. Epub 2020/01/31. doi:
572 10.3389/fnmol.2019.00314. PubMed PMID: 31998072; PubMed Central PMCID:
573 PMCPMC6965019.

574 26. Gooshe M, Abdolghaffari AH, Gambuzza ME, Rezaei N. The role of Toll-like
575 receptors in multiple sclerosis and possible targeting for therapeutic purposes. Rev
576 Neurosci. 2014;25(5):713-39. Epub 2014/06/11. doi: 10.1515/revneuro-2014-0026.
577 PubMed PMID: 24914714.

578 27. Takeuchi O, Sato S, Horiuchi T, Hoshino K, Takeda K, Dong Z, et al. Cutting
579 edge: role of Toll-like receptor 1 in mediating immune response to microbial

580 lipoproteins. J Immunol. 2002;169(1):10-4. Epub 2002/06/22. doi:
581 10.4049/jimmunol.169.1.10. PubMed PMID: 12077222.

582 28. Daniele SG, Beraud D, Davenport C, Cheng K, Yin H, Maguire-Zeiss KA.
583 Activation of MyD88-dependent TLR1/2 signaling by misfolded alpha-synuclein, a
584 protein linked to neurodegenerative disorders. Sci Signal. 2015;8(376):ra45. Epub
585 2015/05/15. doi: 10.1126/scisignal.2005965. PubMed PMID: 25969543; PubMed
586 Central PMCID: PMCPMC4601639.

587 29. Lalive PH, Benkhoucha M, Tran NL, Kreutzfeldt M, Merkler D, Santiago-Raber
588 ML. TLR7 signaling exacerbates CNS autoimmunity through downregulation of Foxp3+
589 Treg cells. Eur J Immunol. 2014;44(1):46-57. Epub 2013/09/11. doi:
590 10.1002/eji.201242985. PubMed PMID: 24018482.

591 30. Dieu RS, Wais V, Sorensen MZ, Marczynska J, Dubik M, Kavan S, et al. Central
592 Nervous System-Endogenous TLR7 and TLR9 Induce Different Immune Responses
593 and Effects on Experimental Autoimmune Encephalomyelitis. Front Neurosci.
594 2021;15:685645. Epub 2021/07/03. doi: 10.3389/fnins.2021.685645. PubMed PMID:
595 34211367; PubMed Central PMCID: PMCPMC8241214.

596 31. Trevino TN, Almousawi AA, Martins-Goncalves R, Ochoa-Raya A, Robinson KF,
597 Abad GL, et al. A Brain Endothelial Cell Caveolin-1/CXCL10 Axis Promotes T Cell
598 Transcellular Migration Across the Blood-Brain Barrier. ASN Neuro.
599 2025;17(1):2472070. Epub 2025/03/10. doi: 10.1080/17590914.2025.2472070. PubMed
600 PMID: 40063988; PubMed Central PMCID: PMCPMC12047051.

601 32. Blandford SN, Fudge NJ, Moore CS. CXCL10 Is Associated with Increased
602 Cerebrospinal Fluid Immune Cell Infiltration and Disease Duration in Multiple Sclerosis.
603 Biomolecules. 2023;13(8). Epub 2023/08/26. doi: 10.3390/biom13081204. PubMed
604 PMID: 37627269; PubMed Central PMCID: PMCPMC10452246.

605 33. Sorensen TL, Trebst C, Kivisakk P, Klaege KL, Majmudar A, Ravid R, et al.
606 Multiple sclerosis: a study of CXCL10 and CXCR3 co-localization in the inflamed central
607 nervous system. J Neuroimmunol. 2002;127(1-2):59-68. Epub 2002/06/05. doi:
608 10.1016/s0165-5728(02)00097-8. PubMed PMID: 12044976.

609 34. Ajami B, Bennett JL, Krieger C, McNagny KM, Rossi FM. Infiltrating monocytes
610 trigger EAE progression, but do not contribute to the resident microglia pool. Nat
611 Neurosci. 2011;14(9):1142-9. Epub 2011/08/02. doi: 10.1038/nn.2887. PubMed PMID:
612 21804537.

613 35. Bailey SL, Schreiner B, McMahon EJ, Miller SD. CNS myeloid DCs presenting
614 endogenous myelin peptides 'preferentially' polarize CD4+ T(H)-17 cells in relapsing
615 EAE. Nat Immunol. 2007;8(2):172-80. Epub 2007/01/09. doi: 10.1038/ni1430. PubMed
616 PMID: 17206145.

617 36. Ifergan I, Kebir H, Bernard M, Wosik K, Dodelet-Devillers A, Cayrol R, et al. The
618 blood-brain barrier induces differentiation of migrating monocytes into Th17-polarizing
619 dendritic cells. Brain. 2008;131(Pt 3):785-99. Epub 2007/12/25. doi:
620 10.1093/brain/awm295. PubMed PMID: 18156156.

621 37. Codarri L, Greter M, Becher B. Communication between pathogenic T cells and
622 myeloid cells in neuroinflammatory disease. Trends Immunol. 2013;34(3):114-9. Epub
623 2012/11/03. doi: 10.1016/j.it.2012.09.007. PubMed PMID: 23116549.

624 38. Yednock TA, Cannon C, Fritz LC, Sanchez-Madrid F, Steinman L, Karin N.
625 Prevention of experimental autoimmune encephalomyelitis by antibodies against alpha
626 4 beta 1 integrin. Nature. 1992;356(6364):63-6. Epub 1992/03/05. doi:
627 10.1038/356063a0. PubMed PMID: 1538783.

628 39. David L, Borges JP, Hollingsworth LR, Volchuk A, Jansen I, Garlick E, et al.
629 NINJ1 mediates plasma membrane rupture by cutting and releasing membrane disks.
630 Cell. 2024;187(9):2224-35 e16. Epub 2024/04/14. doi: 10.1016/j.cell.2024.03.008.
631 PubMed PMID: 38614101; PubMed Central PMCID: PMCPMC11055670.

632 40. Ramos S, Hartenian E, Santos JC, Walch P, Broz P. NINJ1 induces plasma
633 membrane rupture and release of damage-associated molecular pattern molecules
634 during ferroptosis. EMBO J. 2024;43(7):1164-86. Epub 2024/02/24. doi:
635 10.1038/s44318-024-00055-y. PubMed PMID: 38396301; PubMed Central PMCID:
636 PMCPMC10987646.
637

638 **FIGURES LEGENDS**

639

640 **Figure 1. Ninjurin-1 is highly expressed on myeloid cells in the CNS throughout**
641 **RR-EAE.** RR-EAE was induced in female SJL/J mice using $PLP_{139-151}$ emulsified in
642 complete Freund's adjuvant. Spleen and CNS tissues were collected at defined disease
643 stages and analyzed for Ninjurin-1 expression by flow cytometry. (**A**) RR-EAE clinical
644 disease course (n = 8). (**B**) $CD45^{hi}$ $B220^{-}$ $CD3^{-}$ $CD11b^{+}$ infiltrating myeloid cells in the
645 CNS displayed a marked increase in Ninjurin-1 expression compared with splenic myeloid
646 cells at all disease stages (pre-onset, onset, peak, remission, and relapse). (**C**) $CD45^{hi}$
647 $CD3^{+}$ $CD11b^{-}$ T cells in the CNS displayed consistently low Ninjurin-1 expression, with no
648 significant differences compared to splenic $CD3^{+}$ T cells at any disease stage. (**D**)
649 Ninjurin-1 expression in CNS-infiltrating myeloid cells peaked at disease onset and
650 remained elevated at the peak phase. All time points include n = 4 mice, except relapse
651 (n = 3). Data are representative of two independent EAE experiments. Results are shown
652 as mean ± SEM and were analyzed using two-way ANOVA (*$p < 0.05$, **$p < 0.01$, ***$p <$
653 0.001).

654

655 **Figure 2. Inflammatory conditions increase Ninjurin-1 expression on BBB**
656 **endothelial and myeloid cells.** Primary brain microvascular endothelial cells (BBB-ECs)
657 and splenic myeloid cells were cultured for 24 hours under resting conditions or in the
658 presence of inflammatory cytokines to assess Ninjurin-1 expression by flow cytometry.
659 (**A**) BBB-ECs upregulated Ninjurin-1 expression following stimulation with TH1-like (IFN-
660 γ + TNF-α) or TH17-like (GM-CSF + IL-17) cytokine combinations (n = 5 independent

661 experiments). (**B**) $CD45^+$ $CD11b^+$ $Ly6G^-$ myeloid cells isolated from spleens of naïve
662 C57BL/6 mice exhibited increased Ninjurin-1 expression when stimulated with GM-CSF,
663 TNF-α, or TH1-/TH17-like cytokine conditions (n = 6 independent experiments). Data are
664 presented as mean ± SEM and analyzed using two-way ANOVA (*$p < 0.05$, **$p < 0.01$,
665 ***$p < 0.001$).
666
667 **Figure 3. Ninjurin-1^+ myeloid cells exhibit enhanced activation and inflammatory**
668 **cytokine expression in the CNS.** $CD45^{hi}$ $B220^-$ $CD11b^+$ infiltrating myeloid cells were
669 isolated from the CNS of SJL/J mice at disease onset during RR-EAE and analyzed by
670 flow cytometry. (**A**) Ninjurin-1^+ myeloid cells (open squares) displayed significantly higher
671 expression of the co-stimulatory molecules CD80 and CD86, as well as MHC class II,
672 compared with Ninjurin-1^- counterparts (closed circles). (**B**) Ninjurin-1^+ myeloid cells also
673 exhibited increased expression of the inflammatory cytokines TNF-α, IL-1β, and IL-12p40.
674 Data represent n = 5 mice and are presented as mean ± SEM. Statistical significance was
675 determined using paired t-test (*$p < 0.05$, **$p < 0.01$).
676
677 **Table 1. List of genes differentially expressed between Ninjurin-1^+ and Ninjurin-1^-**
678 **myeloid cells.** Shown are genes with their corresponding fold-regulation values and *p*-
679 values comparing Ninjurin-1^+ versus Ninjurin-1^- $CD45^+CD11b^+B220^-CD3^-Ly6G^-$ myeloid
680 cells, as determined by RT^2 Profiler PCR Array analysis.
681 † Only genes showing ≥1.5-fold difference between groups are represented. Positive
682 values indicate upregulation in Ninjurin-1^+ cells relative to Ninjurin-1^- cells.

683 †† *p*-values were calculated using a Student's *t*-test on replicate 2^(−ΔCT) values for each
684 gene in the Ninjurin-1^{+} and Ninjurin-1^{-} groups (*n* = 3 independent experiments).
685
686 **Figure 4. Ninjurin-1^{+} myeloid cells enhance CD4^{+} T cell activation and cytokine**
687 **production.** CD45^{+} B220^{-} CD3^{-} CD11b^{+} Ly6G^{-} Ninjurin-1^{+} or Ninjurin-1^{-} myeloid cells
688 were flow-sorted and co-cultured with CFSE-labeled CD4^{+} T cells isolated from 2D2 mice.
689 Cells were stimulated with MOG_{35-55} peptide in 96-well plates for 72 hours. (**A**) T cell
690 proliferation, measured by CFSE dilution, was greater when CD4^{+} T cells were co-
691 cultured with Ninjurin-1^{+} myeloid cells compared to Ninjurin-1^{-} cells. Controls included
692 CD4^{+} T cells cultured without antigen-presenting cells (APCs) or without MOG_{35-55}
693 peptide. (**B**) CD4^{+} T cells co-cultured with Ninjurin-1^{+} myeloid cells showed increased
694 expression of CD25 and TNF-α, indicating higher levels of activation and inflammatory
695 cytokine production. Data represent n = 4 independent experiments and are shown as
696 mean ± SEM. Statistical analysis was performed using two-way ANOVA (*p < 0.05, **p ≤
697 0.01, ***p < 0.001).
698
699 **Figure 5. Anti-Ninj$_{26–37}$ treatment at peak RR-EAE protects against relapse and**
700 **reduces CNS immune cell infiltration.** RR-EAE was induced in SJL/J mice by
701 subcutaneous injection of $PLP_{139-151}$ emulsified in CFA. Mice were treated
702 intraperitoneally three times per week with anti-Ninj$_{26–37}$ peptide (1 mg/mL; n = 11) or
703 scramble control (n = 11), starting at the peak of disease (day 15) and continuing until
704 day 30 post-induction. (**A**) Anti-Ninj$_{26–37}$–treated mice (open circles) displayed
705 significantly reduced clinical scores and were protected from relapse compared with

706 scramble-treated controls (closed squares; ***$p < 0.001$ by Mann–Whitney test). (**B**) Flow
707 cytometry of CNS mononuclear cells showed a marked reduction in total $CD45^{hi}$
708 leukocytes, including $CD3^+$ T cells, $CD4^+$ T cells, $B220^+$ B cells, and $CD11b^+$ myeloid
709 cells, in anti-$Ninj_{26–37}$–treated mice ($n = 5$; *$p < 0.05$ by multiple unpaired t-tests).
710 (**C**) Representative H&E-stained spinal cord sections collected at day 30 show reduced
711 inflammatory infiltrates in anti-$Ninj_{26–37}$–treated mice compared to controls. Data are
712 representative of at least three sections per mouse from four mice per group. Scale bar
713 = 200 μm. (**D**) Cellular infiltration was quantified by counting hematoxylin-positive nuclei
714 within standardized 300 × 300 μm white matter regions (three ROIs per section, averaged
715 per mouse) and expressed as cells per mm^2. Each dot represents one mouse; bars
716 indicate mean ± SEM.

Figure 1

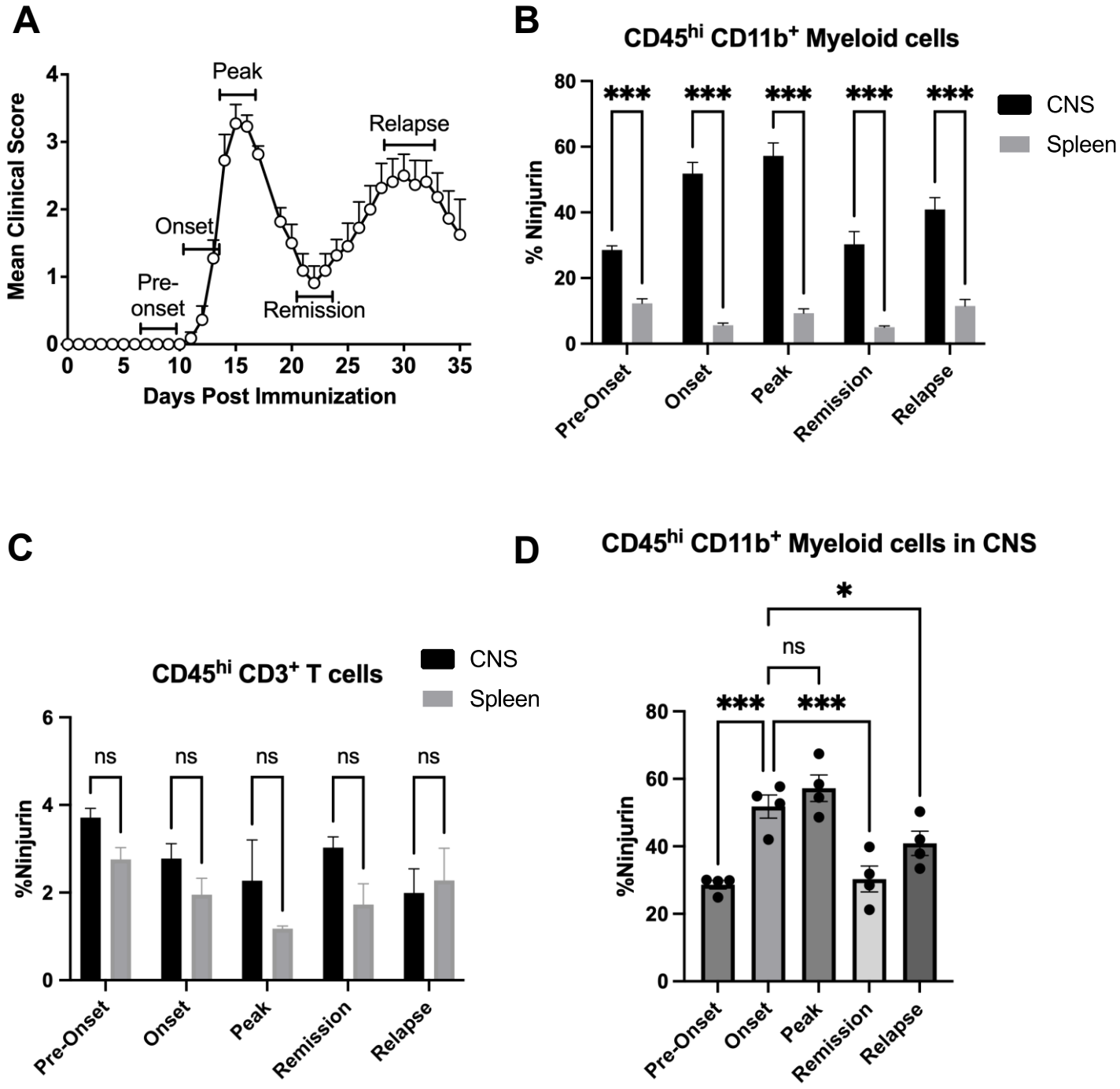
A
Mean Clinical Score
Days Post Immunization
Peak
Relapse
Onset
Pre-
onset
Remission
B
CD45hi CD11b+ Myeloid cells
% Ninjurin
CNS
Spleen
***
Pre-Onset
Onset
Peak
Remission
Relapse
C
CD45hi CD3+ T cells
%Ninjurin
CNS
Spleen
ns
Pre-Onset
Onset
Peak
Remission
Relapse
D
CD45hi CD11b+ Myeloid cells in CNS
%Ninjurin
*
ns
***
Pre-Onset
Onset
Peak
Remission
Relapse

Figure 2

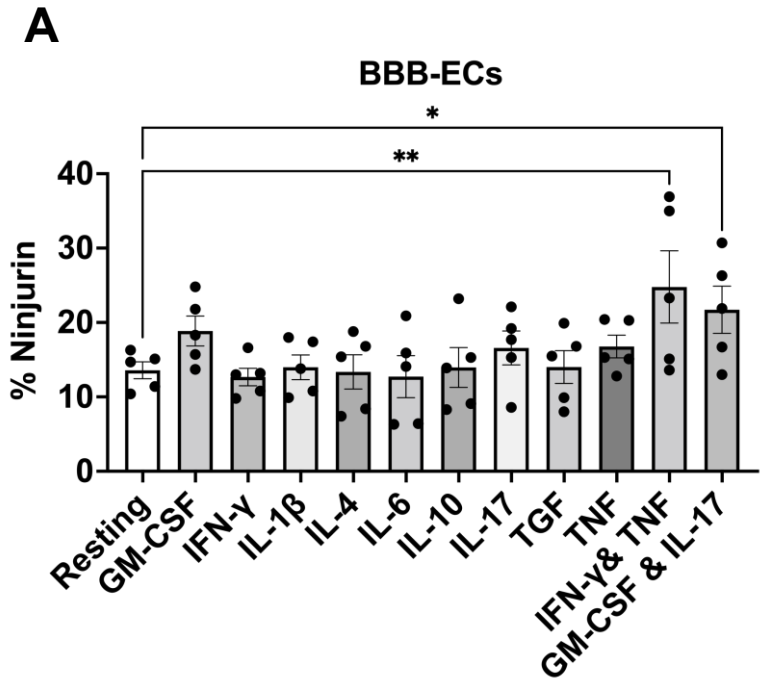
A
BBB-ECs
*
**
% Ninjurin
40
30
20
10
0
Resting
GM-CSF
IFN-γ
IL-1β
IL-4
IL-6
IL-10
IL-17
TGF
TNF
IFN-γ& TNF
GM-CSF & IL-17

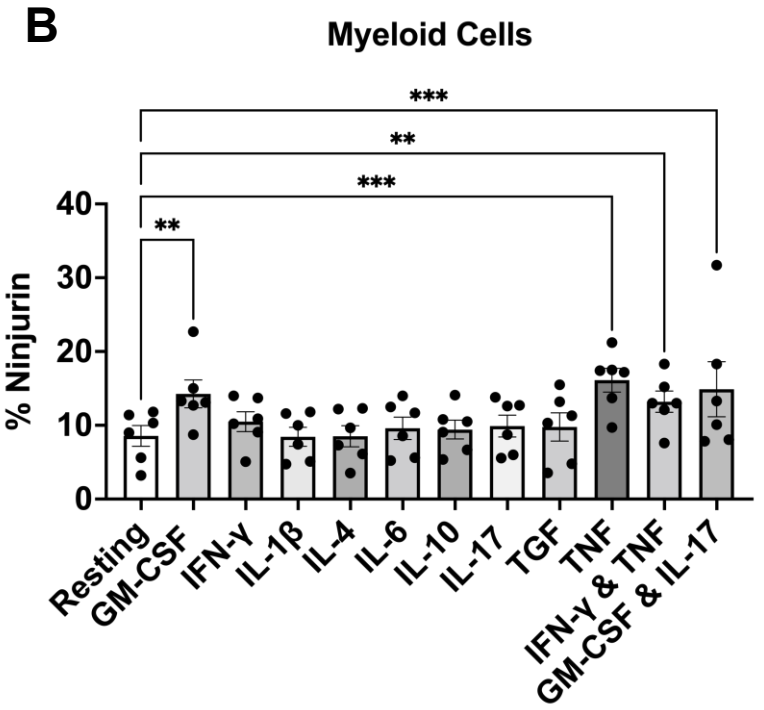
B
Myeloid Cells
***
**
***
**
% Ninjurin
40
30
20
10
0
Resting
GM-CSF
IFN-γ
IL-1β
IL-4
IL-6
IL-10
IL-17
TGF
TNF
IFN-γ & TNF
GM-CSF & IL-17

Figure 3

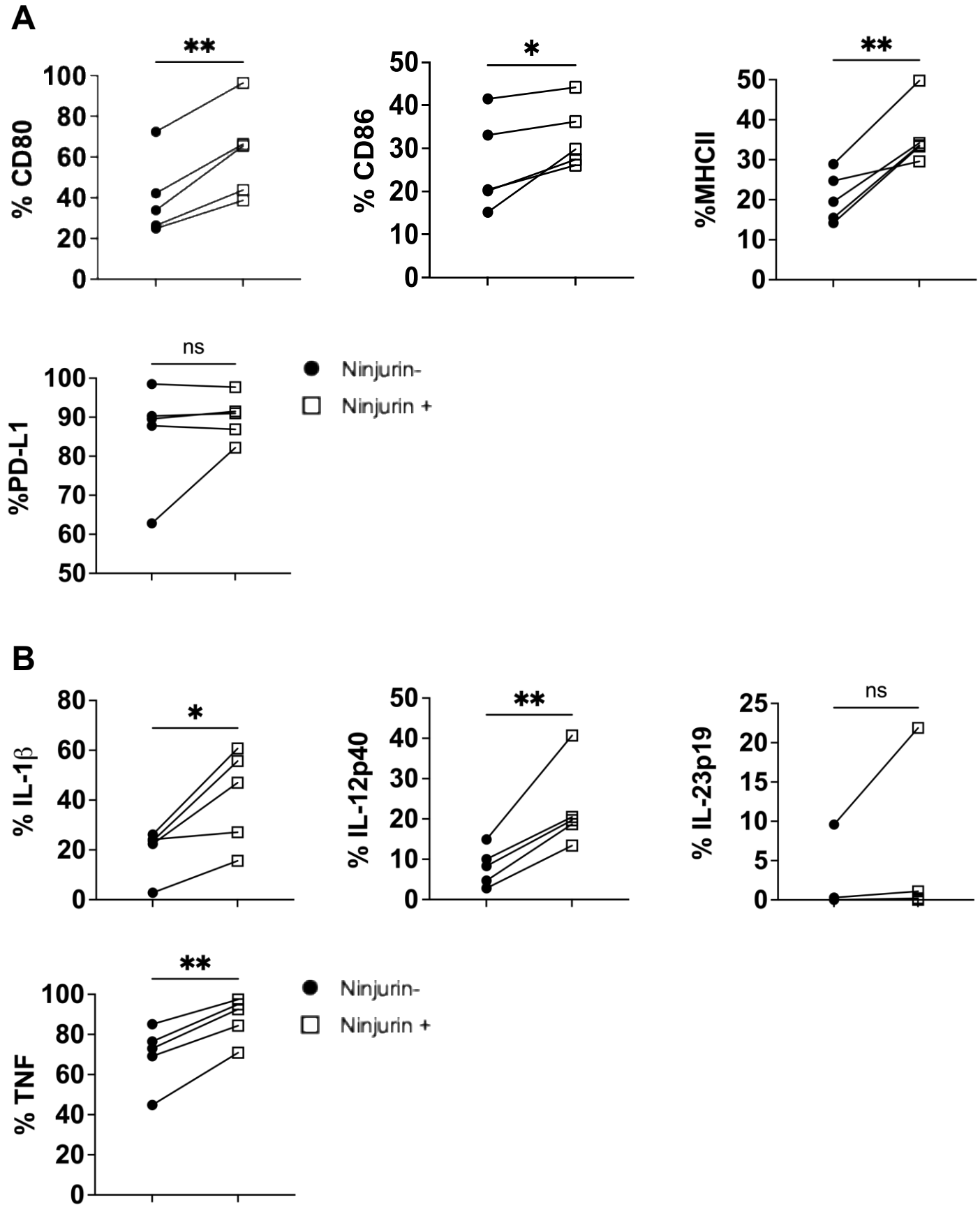
A
**
% CD80
100
80
60
40
20
0
*
% CD86
50
40
30
20
10
0
**
%MHCII
50
40
30
20
10
0
ns
%PD-L1
100
90
80
70
60
50
Ninjurin-
Ninjurin +
B
*
% IL-1β
80
60
40
20
0
**
% IL-12p40
50
40
30
20
10
0
ns
% IL-23p19
25
20
15
10
5
0
**
% TNF
100
80
60
40
20
0
Ninjurin-
Ninjurin +

Table 1: List of genes differentially expressed between Ninjurin-1^{+} and Ninjurin-1^{-} myeloid cells

Gene Symbol	Fold Regulation†	p-value††
Lrp1	6.04	0.006112
Fcgrt	4.59	0.016751
Tlr1	4.49	0.025853
Relb	3.85	0.037913
Cd40	3.59	0.025442
Csf1r	3.12	0.035088
Icam1	3.01	0.035127
Cxcl10	2.87	0.023356
Tlr7	2.57	0.009076
Lyn	2.49	0.023053
Cd44	2.47	0.000941
H2-DMa	2.14	0.024490
Thbs1	2.04	0.045327
Tnf	2.03	0.024954
Itgam	1.55	0.003831
Ccl3	-6.20	0.048783
Ccl4	-10.16	0.008899
Ccl5	-29.53	0.003971

Figure 4

A

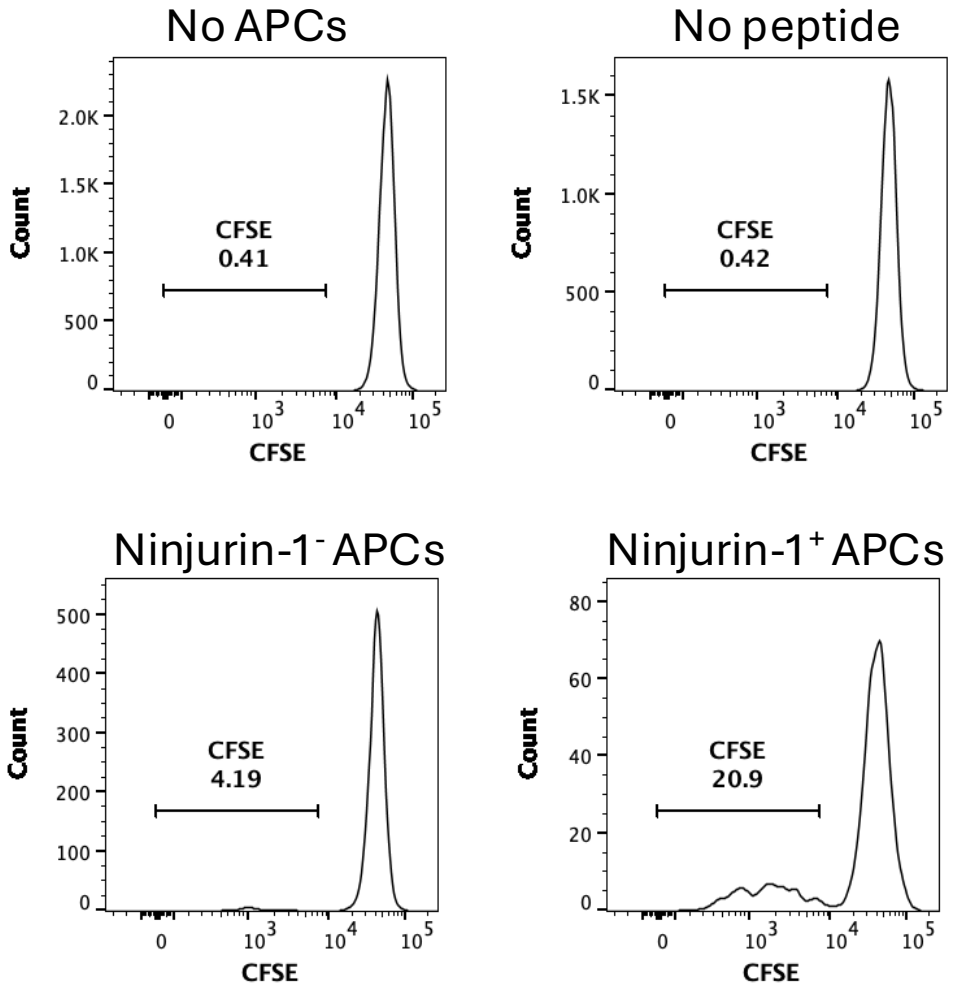
No APCs
No peptide
Ninjurin-1⁻ APCs
Ninjurin-1⁺ APCs
Count
CFSE
CFSE 0.41
CFSE 0.42
CFSE 4.19
CFSE 20.9

B

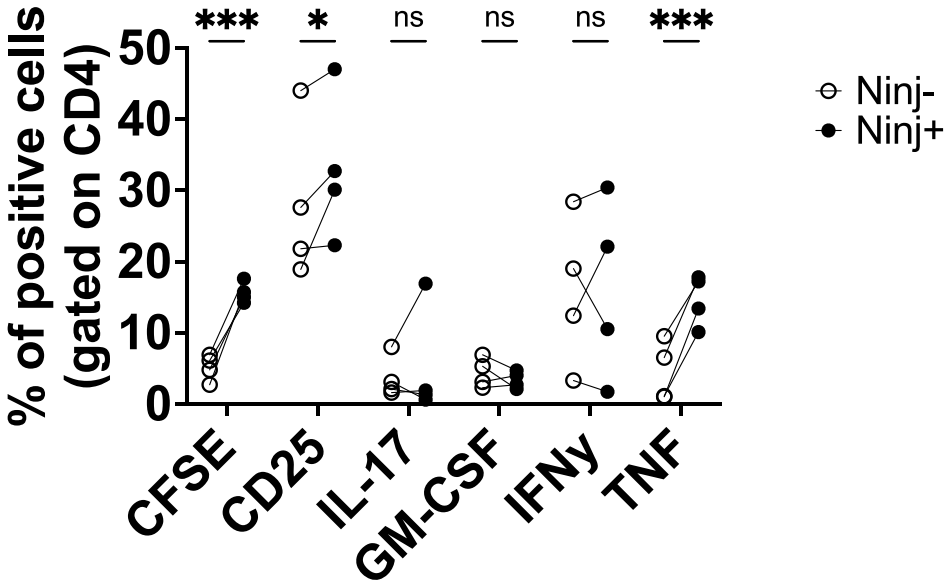
% of positive cells (gated on CD4)
***
*
ns
ns
ns
***
Ninj-
Ninj+
CFSE
CD25
IL-17
GM-CSF
IFNγ
TNF

Figure 5

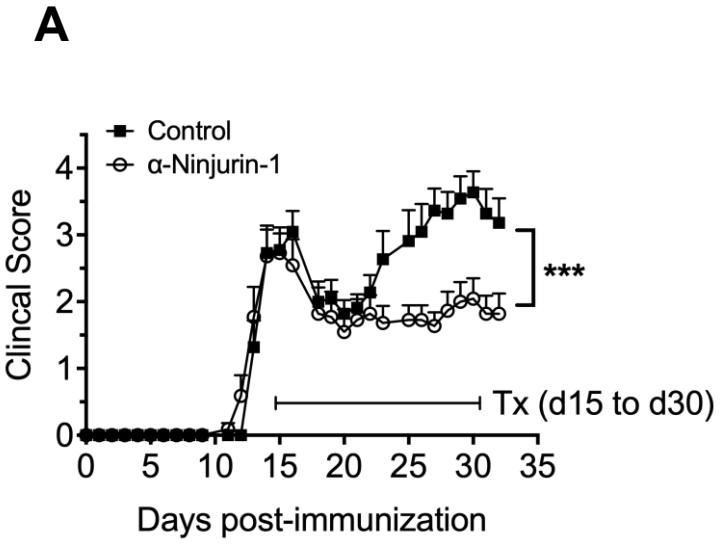
A
Control
α-Ninjurin-1
Clincal Score
Days post-immunization
***
Tx (d15 to d30)

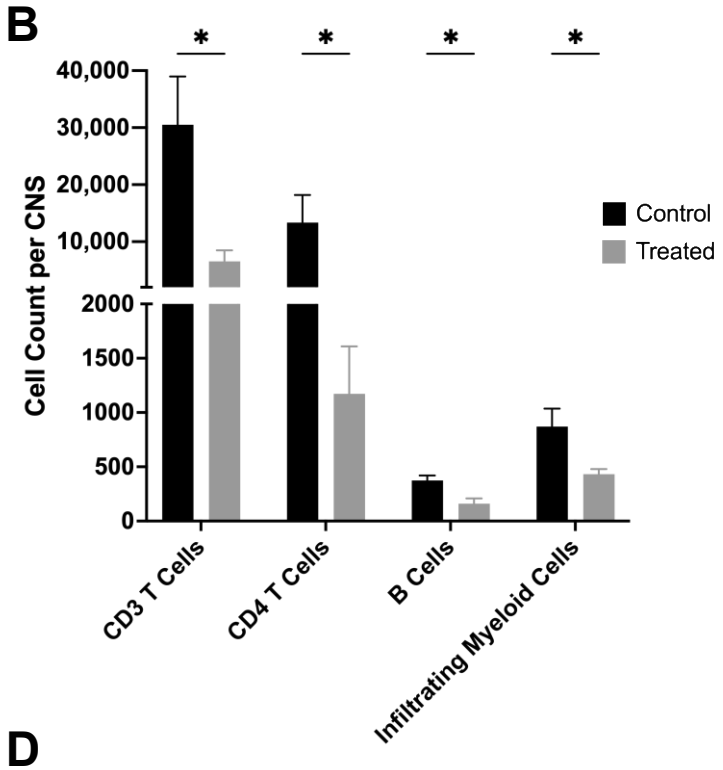
B
Cell Count per CNS
Control
Treated
CD3 T Cells
CD4 T Cells
B Cells
Infiltrating Myeloid Cells

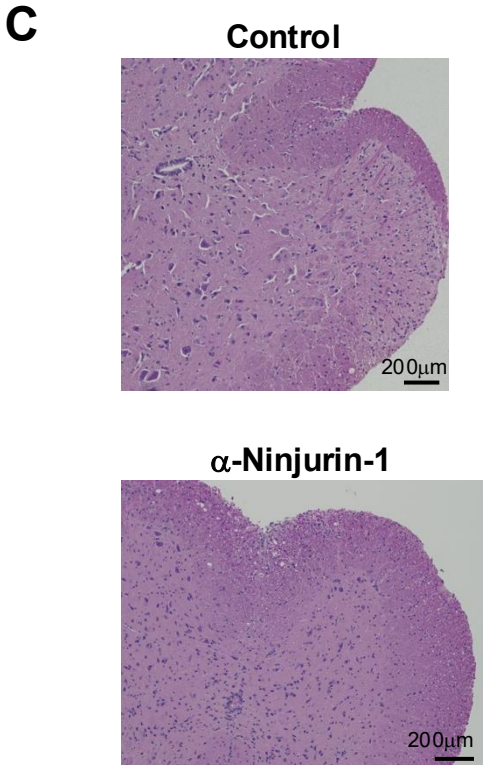
C
Control
200μm
α-Ninjurin-1
200μm

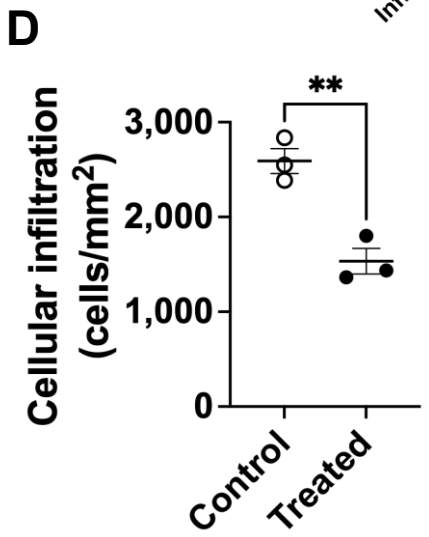
D
Cellular infiltration (cells/mm2)
**
Control
Treated